Carbohydrate Polymers 109 (2014) 28–34

Contents lists available at ScienceDirect

Carbohydrate Polymers

journal homepage: www.elsevier.com/locate/carbpol

Preparation and biological evaluation of a novel selenium-containing exopolysaccharide from *Rhizobium* sp. N613

Guo-Bin Ding[a,1], Rui-Hong Nie[a,1], Li-Hua Lv[a], Guo-Qin Wei[b], Liang-Qi Zhao[a,*]

[a] *Institute of Biotechnology, The Key Laboratory of Chemical Biology and Molecular Engineering of Ministry of Education, Shanxi University, Taiyuan 030006, People's Repubic of China*
[b] *Shanxi Jincheng Anthracite Mining Group Co., Ltd., Jincheng 048006, People's Repubic of China*

ARTICLE INFO

Article history:
Received 19 January 2014
Received in revised form 10 February 2014
Accepted 5 March 2014
Available online 27 March 2014

Keywords:
Selenium-containing exopolysaccharide
Response surface methodology (RSM)
Antitumor activity
Immunomodulatory effect

ABSTRACT

In order to obtain a low toxic antitumor agent and an organic selenium source, an exopolysaccharide obtained from *Rhizobium* sp. N613 (REPS) was modified by selenious acid using barium chloride as the catalyst. The reaction conditions were optimized by response surface methodology (RSM), and the optimal conditions for preparation of selenium-containing REPS (Se-REPS) were obtained. The selenium content of Se-REPS was 790 μg/g under these conditions. The molecular structure of Se-REPS was confirmed by FTIR. In vitro antitumor activity of Se-REPS was evaluated by MTT assay, and the results indicated that Se-REPS could significantly inhibit the growth of S180 and HepG2 cells. Furthermore, Se-REPS exhibited comparable in vivo antitumor efficacy to cyclophosphamide at same concentrations. In addition, Se-REPS could substantially elevate the thymus and spleen indices in tumor-bearing mice. This study demonstrates that Se-REPS holds great potential to be a desirable antitumor agent for therapeutic and immunomodulatory applications.

1. Introduction

Selenium (Se) is an essential trace element for human beings and it is of great biological significance in several enzymes, such as glutathione peroxidase, thioredoxin reductase, and iodothyronine deiodinase (Avila et al., 2013; Liu et al., 2013; Qiu et al., 2014). In addition to being a vital structural component of some enzymes, it has been shown that selenium plays a key role in a number of important biological processes including cancer development, cardiovascular disease, immune function, aging, and so on (Eaton, Abdul Baki, Waring, Roberts, & Lu, 2010; El-Bayoumy, 2001; Kryukov et al., 2003; Méplan, 2011; Rezaei & Dalir-Naghadeh, 2009).

Selenium compounds have drawn extensive attention in recent years due to the important biological activities of selenium. The toxicology and pharmacology of some selenium compounds have been widely studied and the results show that the chemical form of selenium is important (Abdel-Tawwab, Mousa, & Abbass, 2007; Li & Wang, 2004; Sinha, Said, & Medina, 1996; Wang & Lovell, 1997). It is commonly believed that the organic selenium compounds are better and safer than the inorganic selenium ones and can serve as the suitable Se dietary supplements for human to keep healthy or treat related diseases. Thus, it is critical to develop organic Se dietary sources for human beings (Shang, Zhang, Wen, Li, & Cui, 2009; Wang, Zhao, Wang, Yao, & Zhang, 2012a).

Polysaccharides are available from plants, animals or microorganisms, and bacteria can secrete various exopolysaccharides (EPS) (Cheng et al., 2014; Mata et al., 2006; Rana, Das, Gogoi, & Kumar, 2014; Zong, Cao, & Wang, 2012). EPS is a biomacromolecule that is produced by metabolic pathways of microorganisms including bacteria and fungi (Chen, Yan, Zhu, & Xu, 2011; Guo et al., 2013). As an important structural component of all organisms, exopolysaccharides participate in energy transfer, and thus affect a wide range of processes including signal recognition, cellular development and differentiation, as well as immune regulation. Recently, selenized polysaccharides have aroused worldwide concern because of their significant biological activities. It has been reported that selenium-containing polysaccharides exhibited strong anti-diabetic effect, antioxidant property, antitumor and immune-enhancing activity (Jin, Lu, Huang, Wang, & Wang, 2012; Qin et al., 2013; L. Wang et al., 2011; W.F. Wang et al., 2013). However, only limited information about the selenium-containing expolysaccharides is available until now.

In our previous study, a *Rhizobium* sp. N613 exopolysaccharide (REPS) was reported for the first time, which is about 35 kD and

* Corresponding author. Tel.: +86 351 7017663; fax: +86 351 7011499.
E-mail address: liangqi@sxu.edu.cn (L.-Q. Zhao).
[1] These authors contributed equally to this work.

http://dx.doi.org/10.1016/j.carbpol.2014.03.038
0144-8617/

possesses antitumor and antioxidant effects (Zhao, Chen, Ren, Han, & Cheng, 2010). To further improve the biological properties of REPS and obtain an ideal organic Se source, herein, a novel selenium-containing *Rhizobium* sp.N613 expolysaccharide—Se-REPS was synthesized and the preparation conditions were optimized by response surface methodology (RSM). In an attempt to demonstrate the potential application of Se-REPS in tumor chemotherapy, the antitumor activity and immunomodulatory effect were examined, and the results were inspiring: Se-REPS could obviously suppress tumor growth both in vitro and in vivo, and dramatically increase the thymus and spleen indices in S180-bearing mice. These promising results demonstrated that Se-REPS could serve as an effective and safe antitumor agent for chemotherapy.

2. Materials and methods

2.1. Major materials

REPS (≥97%) is prepared according to our previous study (Zhao et al., 2010). Selenious acid and sodium selenite were purchased from Tianjin Chemical Reagent Factory. Cyclophosphamide (CTX) was obtained from (Jiangsu Hengrui Medicament, China), and thiazolyl blue tetrazolium bromide (MTT, ~98%) was purchased from Sigma. All other organic solvents used were of analytical grade.

2.2. Animals and cell lines

Specific pathogen-free (SPF) Kunming mice (male, 19.0–21.0 g) were purchased from the Animal Research Center of Shanxi Medical University. Cell lines of sarcoma 180 (S180) and hepatocarcinoma (HepG2) were purchased from the Animal Research Center of Shanxi Tumor Hospital.

2.3. Preparation of Se-REPS

Solution A was prepared by adding 0.965 g REPS into 50 mL distilled water and stirred overnight at room temperature. Solution B was obtained by adding 1.2 g selenious acid and 0.92 g barium chloride to Solution A and incubated for 7.2 h at 69 °C, then it was cooled to room temperature. Certain amount of dilute sulfuric acid was added to Solution B, supernatant (Solution C) was collected by centrifugation and pH value was adjusted to 7. The obtained solution was then dialyzed against water for 48 h to remove inorganic ions (Mw cut-off: 3500 Da). Subsequently, ethanol was added, a white material precipitated and was separated by centrifugation. Finally, a white powder of Se-REPS was obtained by lyophilization.

2.4. Establishment of the standard curve of selenium

Sodium selenite was used as the standard molecule. Solutions (25 mL) containing different concentrations of selenium were prepared and their pH values were adjusted to 1.5–2.5 with 1 mol/L hydrochloric acid. 2.0 mL of 1% o-phenylene diamine was added, after reacting for 50 min in the dark, 10 mL of toluene was used to extract selenium, the absorbance at 335 nm was determined and the standard curve was plotted.

2.5. Determination of selenium content in Se-REPS

50 mg Se-REPS and 6 mL concentrated acid mixture ($HClO_4$:H_2SO_4:HNO_3 = 1:1:4) were added to a beaker and heated until the solution stopped fuming. Then the solution was diluted to 25 mL by distilled water, and the following procedures were the same as described in 2.4. Selenium content in Se-REPS samples was calculated according to the established standard curve above.

2.6. Box–Behnken design

On the basis of single-variable experiments, the Box–Behnken design was used to estimate the model coefficients. The levels of the five independent variables are indicated in Table 1. All calculations and graphics were performed by using the experimental design software Design Expert 8.0.

2.7. FTIR analysis

Fourier transform infrared (FTIR) spectra studies were carried out in the range of 4000–400 cm^{-1} on FTIR 8300 spectrometer (Shimadzu, Japan) using the standard KBr disk method.

2.8. In vitro antitumor study

The in vitro antitumor effect of Se-REPS and sodium selenite was evaluated by an MTT assay using two different cell lines—S180 and HepG2. Cells were seeded in a 96-well plate at a density of 5000 cells/well and incubated in Dulbecco's modified eagle medium (DMEM) (Hyclone) containing 10% fetal bovine serum (FBS) at 37 °C in 5% CO_2 for 24 h. Then, the medium was removed and replaced by Se-REPS and sodium selenite with different selenium concentrations (0.5, 1.0, 2.0, 5.0, 10.0, or 20.0 μmol/L). After treatment for 24 h, the medium was replaced by 100 μL of fresh DMEM, followed by adding 20 μL of MTT solution (5 mg/mL in PBS). After incubation for another 4 h, 150 μL of dimethyl sulfoxide (DMSO) was added to each well and incubated at 37 °C for 10 min. The results were analyzed and recorded on a microplate reader (Bio-rad, USA).

2.9. Evaluation of the in vivo antitumor activity and immunoregulatory effects of Se-REPS

All the animal procedures were strictly carried out in accordance with the PR China legislation on the use and care of laboratory animals. 0.2 mL S180 ascites tumor cells in PBS (1×10^7 cells/mL) were inoculated subcutaneously into the right axilla of each mouse. The mice inoculated with tumor cells were randomly divided into 8 groups and each group having ten mice. Different groups of mice were administrated intraperitoneally with: saline (10 mL/kg, group I, negative control), cyclophosphamide (20 mg/kg, group II, positive control), REPS (5, 10, 20 mg/kg, group III–V), and Se-REPS (5, 10, 20 mg/kg, group VI–VIII), respectively, once a day for a total of ten times. All mice were killed by dislocation of cervical vertebra at day 10 post inoculation and the tumors, spleens and thymuses were collected and weighed. The inhibition rate, spleen index and the thymus index were calculated according to the following equations:

$$\text{Inhibition rate of tumor growth}(\%) = \frac{W_c - W_t}{W_c} \times 100\%,$$

where W_c and W_t are the average tumor weights (mg) of the negative control and the treated mice respectively (Lv et al., 2013).

$$\text{spleen index}(\text{mg/g}) = \frac{W_{\text{spleen}}}{W_{\text{body}}} \times 100\%,$$

where W_{spleen} and W_{body} are the average spleen weights (mg) and average body weights (g) respectively; and:

$$\text{thymus index}(\text{mg/g}) = \frac{W_{\text{thymus}}}{W_{\text{body}}} \times 100\%,$$

where W_{thymus} and W_{body} are the average thymus weights (mg) and average body weights (g) respectively.

Table 1
List of variables and levels for preparation of Se-REPS.

Levels	Variables				
	Concentration of selenious acid (mg/mL)	Concentration of REPS (mg/mL)	Concentration of barium chloride (mg/mL)	Reaction temperature (°C)	Reaction time (h)
1	10	10	12	60	6
2	20	20	18	70	7
3	30	30	24	80	8

2.10. Statistical analysis

The data are expressed as means ± standard deviation (SD). The differences between the control and test groups were tested using Student's *t*-test. Differences were considered statistically significant when $P < 0.05$.

3. Results and discussion

3.1. Analysis of the response surface model

Response surface methodology (RSM) is a powerful statistical technique that is widely used for optimizing a process when the independent variables have a combined effect (Shen et al., 2014). Therefore, it was used to optimize the reaction conditions in this study. Effects of the concentration of selenious acid and REPS (*A* and *B*), concentration of barium chloride (*C*), reaction temperature and reaction time (*D* and *E*) on the selenium content (*Y*) of Se-REPS were studied by Box–Behnken design.

In order to determine whether or not the quadratic model is significant, it is necessary to conduct ANOVA analysis. The coefficient of determination (R^2), adjusted determination coefficient (adj. R^2), coefficients of variation (CV), and *P*-values were used to judge the adequacy of the model and the results are shown in Table 2 (Chen, Chen, Srinivasakannan, & Peng, 2012). The coefficient of determination (R^2) of the model is 0.9475, which indicates that 94.75% of the variability in the dependent variable could be explained, and only 5.25% of the total variations cannot be explained by the model. The value of the adjusted determination coefficient (adj. R^2) is 0.9055, which suggested that there are excellent correlations between the independent variables. The value of CV (4.24%) less than 10% showed a higher degree of precision and better reliability of the experimental values. The smaller the *P*-values are, the bigger the significance of the corresponding coefficient (Li, Cui, Liu, Xu, & Zhao, 2007). Here, the *P*-value of the model was smaller than 0.0001, which indicated that the model was suitable for use in this experiment.

From the results obtained in Table 2, the *A*, *B*, *C*, *D*, *E*, *AB*, *AC*, *CE*, A^2, B^2, C^2, D^2, E^2, were significant model terms. By applying least squares method and multiple regression analysis on the experimental results, the quadratic regression equation can be obtained and shown in the following equation:

$$Y = 791.00 + 36.50A - 25.50B + 16.25C - 34.75D + 17.63E + 52.50AB + 33.75AC + 13.75AD + 10.50AE - 17.25BC + 14.25BD + 22.50BE - 7.00CD + 31.00CE - 1.50DE - 73.58A^2 - 87.08B^2 - 85.58C^2 - 146.75D^2 - 84.75E^2$$

The optimal values of the selected variables were obtained by solving the regression equation using Design-Expert 8.0 software. The optimal conditions for selenium content of Se-REPS estimated by the model equation were as follows, concentration of selenious acid: 24 mg/mL; concentration of REPS: 19.3 mg/mL; concentration of barium chloride: 18.4 mg/mL; reaction temperature: 69 °C; reaction time: 7.2 h. Under these conditions, the measured selenium content of Se-REPS was 790 μg/g, which is well in close agreement with the value predicted by the model. The results suggested that the model of equation is satisfactory and accurate.

The relationships between the experimental variables and the responses are illustrated in three dimensional representations of the response surfaces. These plots are presented in Fig. 1. The 3-D response surface plot shown in Fig. 1(a) gives the selenium content of Se-REPS as a function of concentration of selenious acid and REPS at fixed concentration of barium chloride (18.4 mg/mL), reaction temperature (69 °C) and reaction time (7.2 h), which indicated that the selenium content of Se-REPS increased gradually with the increasing of the concentration of selenious acid from 10 to 24 mg/mL, but beyond 24 mg/mL, the selenium content of Se-REPS decreased slowly with the increase of the concentration of selenious acid, and the selenium content of Se-REPS was found to increase rapidly with the increase of concentration of REPS from 10 to 19.3 mg/mL, then decreased from 19.3 to 30 mg/mL.

Fig. 1(b) shows the 3-D response surface plot at varying concentration of selenious acid and barium chloride at fixed concentration of REPS (19.3 mg/mL), reaction temperature (69 °C) and reaction time (7.2 h). And selenium content of Se-REPS increased rapidly within concentration of selenious acid from 10 to 24 mg/mL, but when beyond 24 mg/mL, the selenium content of Se-REPS decreased rapidly with the increase of the concentration of selenious acid, and the selenium content increased slightly with the increase of concentration of barium chloride from 12 to 18.4 mg/mL, then dropped from 18.4 to 24 mg/mL.

In Fig. 1(c), the 3-D response surface plot was developed for the selenium content of Se-REPS with varying concentration of REPS and reaction time at fixed concentration of selenious acid (24 mg/mL), concentration of barium chloride (18.4 mg/mL) and reaction temperature (69 °C). It indicated that the maximum selenium content of Se-REPS can be achieved when concentration of REPS and reaction time were at the threshold level of 19.3 mg/mL and 7.2 h, respectively.

Fig. 1(d) shows the 3-D response surface plot at varying concentration of REPS and reaction temperature at fixed concentration of selenious acid (24 mg/mL), concentration of barium chloride (18.4 mg/mL) and reaction time (7.2 h). And selenium content of Se-REPS increased rapidly within reaction temperature from 60 to 69 °C, but when beyond 69 °C, the selenium content of Se-REPS reached the plateau region where the selenium content was maximized, and the selenium content increased slightly with the increase of concentration of REPS from 10 to 19.3 mg/mL, then dropped from 19.3 to 30 mg/mL.

A normal probability plot of the residuals is presented in Fig. 2, which shows that the residuals generally fall on a least-square line which is used to estimate the cumulative distribution function for the population. As clearly seen from Fig. 2, the errors are normally distributed and there are almost no serious violations of the assumptions that underlie the analysis (Wu, Yick, Ng, & Yip, 2012). By displaying a good normal distribution, the normality assumptions could be confirmed and the predictive regression model has extracted all information available from the experimental data (Davidson, Balasubramanian, & Tagore, 2008).

Table 2
Analysis of response surface methodology of Se-REPS.

Item	Squared deviations	Degrees of freedom	Mean square	*F* value	*P* value	Significant
Model	3.16E+05	20	15,816.29	22.56	<0.0001	***
A	21,316	1	21,316	30.4	<0.0001	***
B	10,404	1	10,404	14.84	0.0007	***
C	4225	1	4225	6.03	0.0214	*
D	19,321	1	19,321	27.56	<0.0001	***
E	4970.25	1	4970.25	7.09	0.0134	**
AB	11,025	1	11,025	15.72	0.0005	***
AC	4556.25	1	4556.25	6.5	0.0173	*
AD	756.25	1	756.25	1.08	0.309	
AE	441	1	441	0.63	0.4352	
BC	1190.25	1	1190.25	1.7	0.2045	
BD	812.25	1	812.25	1.16	0.2921	
BE	2025	1	2025	2.89	0.1016	
CD	196	1	196	0.28	0.6017	
CE	3844	1	3844	5.48	0.0275	*
DE	9	1	9	0.013	0.9107	
A^2	47,253.88	1	47,253.88	67.39	<0.0001	***
B^2	66,183.33	1	66,183.33	94.39	<0.0001	***
C^2	63,922.97	1	63,922.97	91.17	<0.0001	***
D^2	1.88E+05	1	1.88E+05	268.05	<0.0001	***
E^2	62,684.18	1	62,684.18	89.4	<0.0001	***
Residual	17,528.75	25	701.15			
Lack of fit	17,502.75	20	875.14	168.3	<0.0001	***
Pure error	26	5	5.2			
Cor total	3.34E+05	45				

R^2 = 0.9475, Adj. R^2 = 0.9055, and CV = 4.24%.
* $P < 0.05$.
** $P < 0.01$.
*** $P < 0.001$.

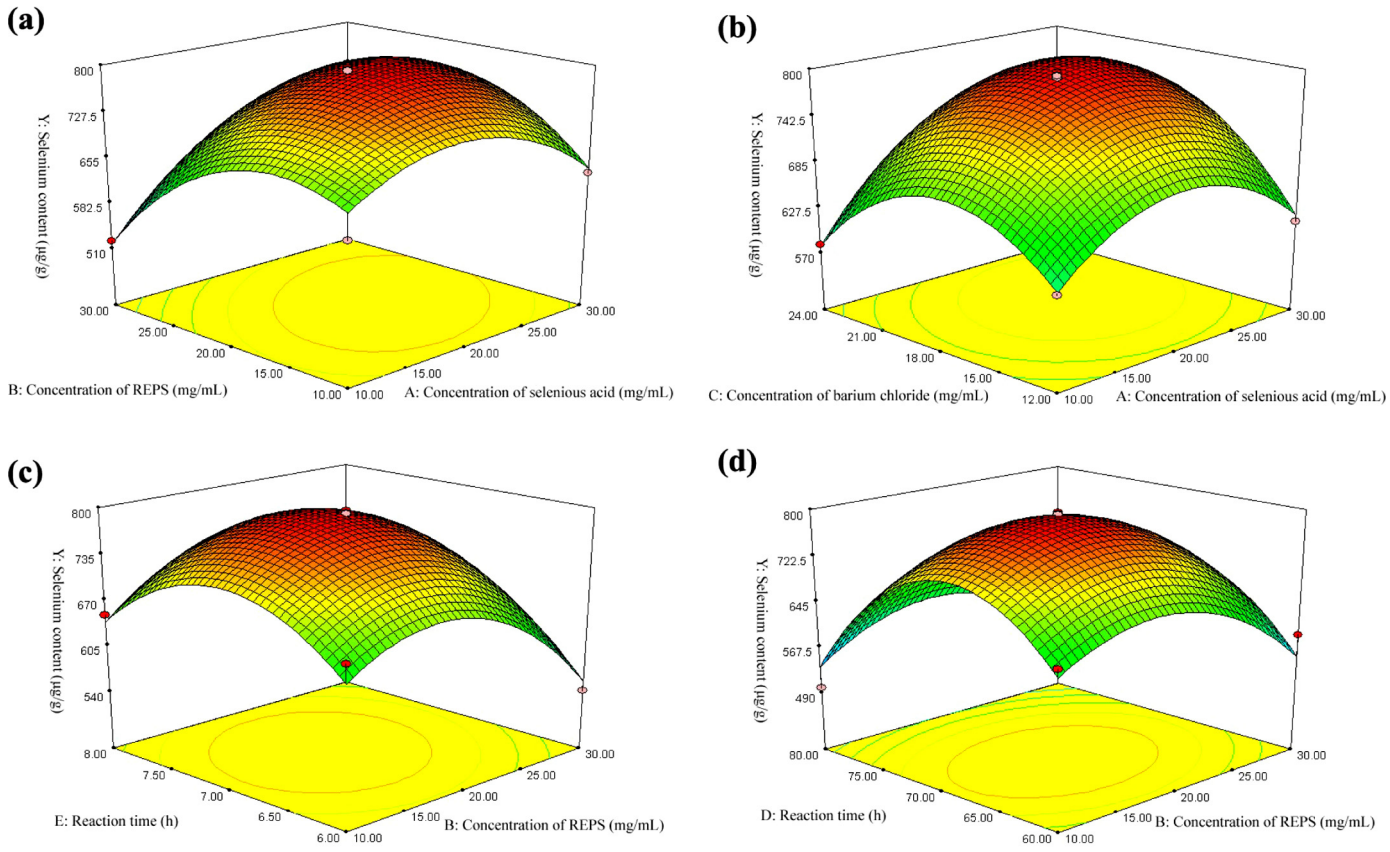

Fig. 1. (a) $Y = f(A, B)$ three-dimensional analysis graphs of the response surface; (b) $Y = f(A, C)$ three-dimensional analysis graphs of the response surface; (c) $Y = f(B, E)$ three-dimensional analysis graphs of the response surface; (d) $Y = f(B, D)$ three-dimensional analysis graphs of the response surface.

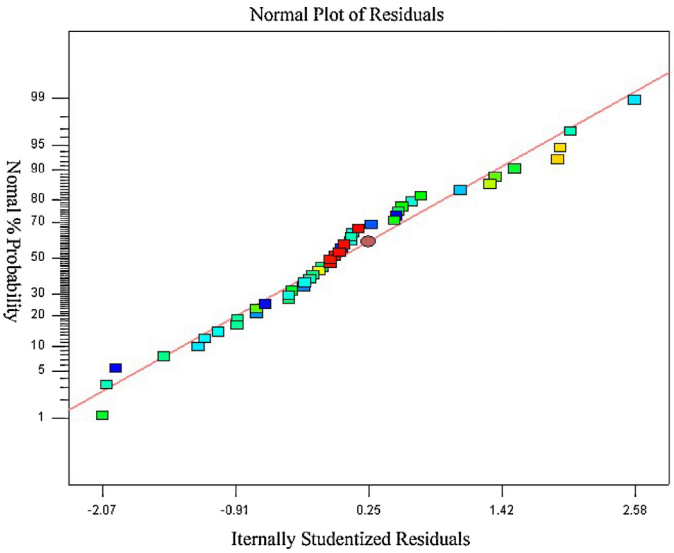

Fig. 2. Normal probability plot of residuals for selenium content of Se-REPS.

3.2. Structural analysis

FTIR was used to investigate and confirm the chemical structure of Se-REPS. Fig. 3 shows the FT-IR spectra for REPS and Se-REPS. It can be seen from Fig. 3 that REPS and Se-REPS have some common characteristic bands: the band observed at 3443 cm^{-1} is assigned to the hydroxyl group; the weak bands at 2923 and 2848 cm^{-1} demonstrating a C—H stretching vibration; the broad bands at 1408 and 1161 cm^{-1} are attributable to C—O stretching vibration; and the peak appeared at 896 cm^{-1} is ascribed to the β-configuration of the sugar units in REPS and Se-REPS. These common peaks suggest that introduction of selenium does not affect the main structure of the polysaccharide (Yu et al., 2009). Furthermore, it is noteworthy that a striking peak observed at 794 cm^{-1} (Fig. 3b) is attributed to the Se=O stretching vibration, which indicating that Se-REPS is successfully synthesized.

3.3. In vitro cytotoxicity study

The inhibition effects of Se-REPS and sodium selenite at various selenium concentrations (ranging from 0.5 to 20.0 μmol/L) against S180 and HepG2 cells were investigated by MTT assay and

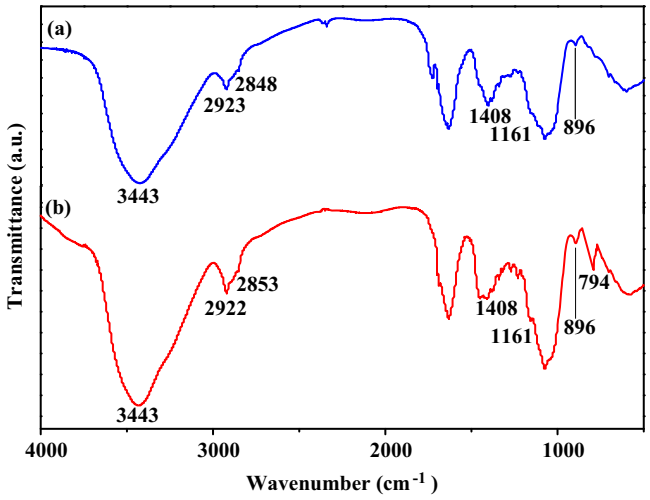

Fig. 3. FTIR spectra of (a) REPS and (b) Se-REPS.

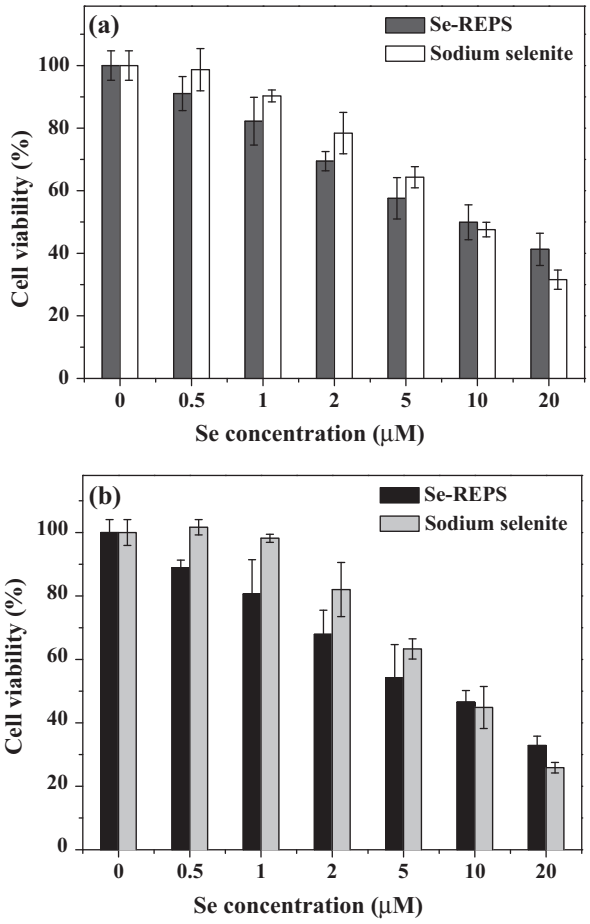

Fig. 4. The cytotoxicity of Se-REPS and sodium selenite against S180 (a) and HepG2 (b) cells as determined by MTT assay. Cells were exposed to Se-REPS and sodium selenite with different selenium concentrations for 24 h. Values are averages of five replicates ± SD (standard deviation).

the results were shown in Fig. 4. As depicted in Fig. 4, both Se-REPS and sodium selenite could significantly inhibit the growth of S180 and HepG2 cells and the antitumor effect was concentration dependent, the highest inhibition rate of Se-REPS and sodium selenite against S180 cells was 58.74 and 68.43% (Fig. 4a), respectively. And for HepG2 cells, that was 67.13 and 74.14% (Fig. 4b), respectively. Moreover, it is easy to see from Fig. 4 that Se-REPS was much more potent than sodium selenite in inhibiting tumor cell growth at lower selenium concentrations (0.5–5 μmol/L), while it was slightly less effective in inhibiting tumor cell growth at higher selenium concentrations (10 and 20 μmol/L). However, it has been reported that sodium selenite is highly toxic to normal cells at high selenium concentrations (Wang et al., 2012b). Taken together, Se-REPS may be a safe and potent antitumor agent.

3.4. In vivo antitumor activities of Se-REPS and REPS against S180-bearing mice

To validate the vital role of selenium played in the antitumor efficacy of Se-REPS, in vivo studies were performed to assess the antitumor effects of Se-REPS and REPS using the sarcoma mice model bearing S180 tumor cells. The tumor formation rate was 100% in this study, and all mice were alive without death during the treatment period. Weight of the excised tumors and the inhibition rate of tumor growth were summarized in Fig. 5. As shown in Fig. 5a, compared to negative control, tumor weight of all treatment groups decreased significantly ($P < 0.05$, 0.01, or 0.0001), that

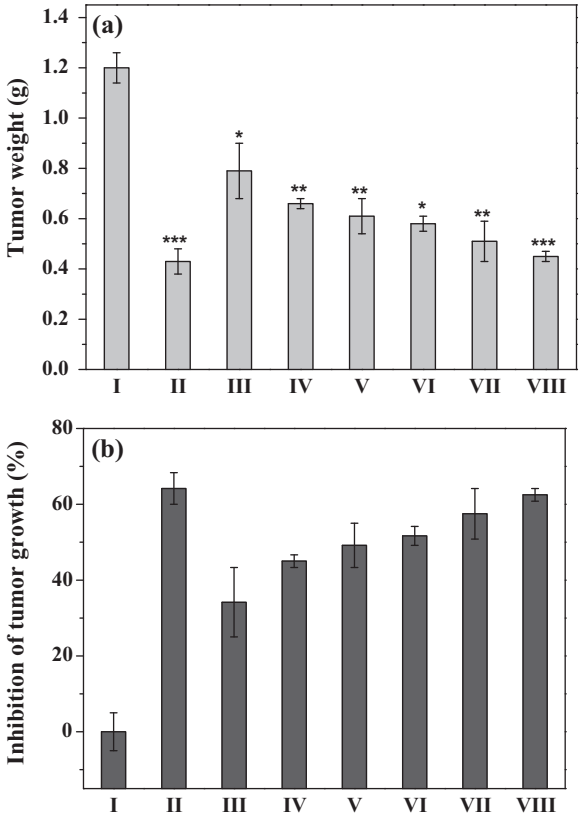

Fig. 5. Tumor weight (a) and inhibition rate of tumor growth (b) in S180 tumor-bearing mice treated with saline (10 mL/kg, I), cyclophosphamide (20 mg/kg, II), REPS (5 mg/kg, III), REPS (10 mg/kg, IV), REPS (20 mg/kg, V), Se-REPS (5 mg/kg, VI), Se-REPS (10 mg/kg, VII), and Se-REPS (20 mg/kg, VIII) once a day. Data are presented as mean ± SD (standard deviations), $n = 10$. $^{*}P < 0.05$, $^{**}P < 0.01$ and $^{***}P < 0.001$ when compared with the saline-treated group.

is, all treatment groups yielded an obvious tumor growth inhibition. Interestingly, Se-REPS exhibited an improved degree of antitumor potency relative to REPS at every tested dose, indicating that selenium may have an important effect on the antitumor activity (Fig. 5). It is worthwhile to note that the group treated with Se-REPS at 20 mg/kg had a higher inhibition rate of 62.5%, which was comparable to that of the positive control group with commercially available cyclophosphamide injection at the same dose (64.2%) (Fig. 5b). Along with the results of in vitro antitumor study, we can reach the conclusion that Se-REPS is a promising antitumor agent and has great potential for cancer therapy.

3.5. The effects of REPS and Se-REPS on the thymus and spleen indices in mice

Spleen and thymus are among the primary immune organs and directly affect the organism's immune function (Guo et al., 2013). It has been reported that selenized polysaccharides could remarkably improve the cellular and humoral immune response in mice (Xu, Wang, Jin, & Yang, 2009). Therefore, to assess the effect of REPS and Se-REPS on the immune organs, the spleen and thymus indices were examined. As presented in Table 3, the thymus and spleen indices were significantly higher in the Se-REPS group and REPS group than in the negative control group ($P < 0.05$, 0.01, or 0.0001), in other words, Se-REPS and REPS greatly improved the weight of the immune organs in S180-bearing mice. Specifically, it is noteworthy that high dose (20 mg/kg) of Se-REPS exhibits the highest thymus and spleen indices. In contrast, the thymus and spleen indices of the positive control group decreased quickly as compared with that of negative control group ($P < 0.01$), supporting the adverse effect of cyclophosphamide on the immune system during the chemotherapy (Cai et al., 2012). Therefore, Se-REPS is a satisfactory immunopotentiator and could markedly enhance the function of immune system in cancer therapy.

Table 3
The effects of REPS and Se-REPS at different doses on the thymus and spleen indices in mice. Results are presented as the mean ± standard deviation ($n = 10$). Negative control: saline; Positive control: cyclophosphamide.

Group	Dose (mg/kg)	Thymus index (mg/g)	Spleen index (mg/g)
Negative control	0	1.52 ± 0.18	7.18 ± 0.35
Positive control	20	0.73 ± 0.07**	6.75 ± 0.32**
REPS	5	1.63 ± 0.09*	7.46 ± 0.12*
	10	1.95 ± 0.08**	7.85 ± 0.16**
	20	1.84 ± 0.14**	7.63 ± 0.08*
Se-REPS	5	1.81 ± 0.05**	7.47 ± 0.17*
	10	1.92 ± 0.08**	7.73 ± 0.18*
	20	2.29 ± 0.08***	8.51 ± 0.15**

* $P < 0.05$ compared with the negative control.
** $P < 0.01$ compared with the negative control.
*** $P < 0.001$ compared with the negative control.

4. Conclusions

In summary, this study presents a facile method to synthesize a novel and efficient low toxic antitumor agent Se-REPS, and the preparation conditions were optimized. Its structure was confirmed by FTIR, characterized by a strong peak detected at 794 cm^{-1} (Se=O stretching vibration). The antitumor efficacy of Se-REPS was evaluated both in vitro and in vivo. The results indicated that Se-REPS could not only effectively suppress the tumor growth but also significantly increase the thymus index and spleen index in tumor-bearing mice, particularly at the high dose of 20 mg/kg. Altogether, the present findings suggest that Se-REPS could be considered as a promising antitumor agent with pronounced immunomodulatory activity.

Acknowledgments

This work was supported by the Science Foundation for Youths of Shanxi Province (No. 2013021014-1) and Scientific Research Starting Foundation of Shanxi University (No. 011351901002).

References

Abdel-Tawwab, M., Mousa, M. A. A., & Abbass, F. E. (2007). Growth performance and physiological response of African catfish, *Clarias gariepinus* (B.) fed organic selenium prior to the exposure to environmental copper toxicity. *Aquaculture, 272*, 335–345.

Avila, F. W., Faquin, V., Yang, Y., Ramos, S. J., Guilherme, L. R. G., Thannhauser, T. W., et al. (2013). Assessment of the anticancer compounds Se-methylselenocysteine and glucosinolates in Se-biofortified broccoli (*Brassica oleracea L. var. italica*) sprouts and florets. *Journal of Agricultural and Food Chemistry, 61*, 6216–6223.

Cai, Z. B., Li, W., Wang, H. T., Yan, W. Q., Zhou, Y. L., Wang, G., et al. (2012). Anti-tumor and immunomodulating activities of a polysaccharide from the root of *Sanguisorba officinalis* L. *International Journal of Biological Macromolecules, 51*, 484–488.

Chen, G., Chen, J., Srinivasakannan, C., & Peng, J. H. (2012). Application of response surface methodology for optimization of the synthesis of synthetic rutile from titania slag. *Applied Surface Science, 258*, 3068–3073.

Chen, H., Yan, M., Zhu, J., & Xu, X. (2011). Enhancement of exo-polysaccharide production and antioxidant activity in submerged cultures of *Inonotus obliquus* by lignocellulose decomposition. *Journal of Industrial Microbiology and Biotechnology, 38*, 291–298.

Cheng, B. H., Chan, J. Y. W., Chan, B. C. L., Lin, H. Q., Han, X. Q., Zhou, X., et al. (2014). Structural characterization and immunomodulatory effect of apolysaccharide HCP-2 from *Houttuynia cordata*. *Carbohydrate Polymers, 103*, 244–249.

Davidson, M. J., Balasubramanian, K., & Tagore, G. R. N. (2008). Surface roughness prediction of flow-formed AA6061 alloy by design of experiments. *Journal of Materials Processing Technology, 202*, 41–46.

Eaton, C. B., Abdul Baki, A. R., Waring, M. E., Roberts, M. B., & Lu, B. (2010). The association of low selenium and renal insufficiency with coronary heart disease and all-cause mortality: NHANES III follow-up study. *Atherosclerosis*, *212*, 689–694.

El-Bayoumy, K. (2001). The protective role of selenium on genetic damage and on cancer. *Mutation Research*, *475*, 123–139.

Guo, Y., Pan, D., Li, H., Sun, Y., Zeng, X., & Yan, B. (2013). Antioxidant and immunomodulatory activity of selenium exopolysaccharide produced by *Lactococcus lactis* subsp. lactis. *Food Chemistry*, *138*, 84–89.

Jin, M. L., Lu, Z. Q., Huang, M., Wang, Y. M., & Wang, Y. Z. (2012). Effects of Se-enriched polysaccharides produced by *Enterobacter cloacae* Z0206 on alloxan-induced diabetic mice. *International Journal of Biological Macromolecules*, *50*, 348–352.

Kryukov, G. V., Castello, S., Novoselov, S. V., Lobanov, A. V., Zehtab, O., Guigó, R., et al. (2003). Characterization of mammalian selenoproteomes. *Science*, *300*, 1439–1443.

Li, Y., Cui, F. J., Liu, Z. Q., Xu, Y. Y., & Zhao, H. (2007). Improvement of xylanase production by *Penicillium oxalicum* ZH-30 using response surface methodology. *Enzyme and Microbial Technology*, *40*, 1381–1388.

Li, J. K., & Wang, X. L. (2004). Effect of dietary organic versus inorganic selenium in laying hens on the productivity, selenium distribution in egg and selenium content in blood, liver and kidney. *Journal of Trace Elements in Medicine and Biology*, *18*, 65–68.

Liu, Y., Sun, J., Rao, S., Su, Y., Li, J., Li, C., et al. (2013). Antidiabetic activity of mycelia selenium-polysaccharide from *Catathelasma ventricosum* in STZ-induced diabetic mice. *Food and Chemical Toxicology*, *62*, 285–291.

Lv, Y., Ding, G., Zhai, J., Guo, Y., Nie, G., & Xu, L. (2013). A superparamagnetic Fe_3O_4-loaded polymeric nanocarrier fortargeted delivery of evodiamine with enhanced antitumor efficacy. *Colloids and Surfaces B: Biointerfaces*, *110*, 411–418.

Mata, J. A., Béjar, V., Llamas, I., Arias, S., Bressollier, P., Tallon, R., et al. (2006). Exopolysaccharides produced by the recently described halophilic bacteria *Halomonas ventosae* and *Halomonas anticariensis*. *Research in Microbiology*, *157*, 827–835.

Méplan, C. (2011). Trace elements and ageing, a genomic perspective using selenium as an example. *Journal of Trace Elements in Medicine and Biology*, *25S*, S11–S16.

Qin, T., Chen, J., Wang, D., Hu, Y., Wang, M., Zhang, J., et al. (2013). Optimization of selenylation conditions for Chinese angelica polysaccharide based on immune-enhancing activity. *Carbohydrate Polymers*, *92*, 645–650.

Qiu, S., Chen, J., Chen, X., Fan, Q., Zhang, C., Wang, D., et al. (2014). Optimization of selenylation conditions for lycium barbarumpolysaccharide based on antioxidant activity. *Carbohydrate Polymers*, *103*, 148–153.

Rana, V., Das, M. K., Gogoi, S., & Kumar, V. (2014). Multifunctional properties of polysaccharides from *Dalbergia sissoo*, *Tectona grandis* and *Mimosa diplotricha*. *Carbohydrate Polymers*, *102*, 341–350.

Rezaei, S. A., & Dalir-Naghadeh, B. (2009). Association of plasma and heart homocysteine and blood malondialdehyde with cardiovascular diseases induced by acute selenium deficiency in lambs. *Small Ruminant Research*, *83*, 22–28.

Shang, D. J., Zhang, J. N., Wen, L., Li, Y., & Cui, Q. (2009). Preparation, characterization, and antiproliferative activities of the Se-containing polysaccharide SeGLP-2B-1 from Se-enriched *Ganoderma lucidum*. *Journal of Agricultural and Food Chemistry*, *57*, 7737–7742.

Shen, S., Chen, D., Li, X., Li, T., Yuan, M., Zhou, Y., et al. (2014). Optimization of extraction process and antioxidant activity of polysaccharides from leaves of *Paris polyphylla*. *Carbohydrate Polymers*, *104*, 80–86.

Sinha, R., Said, T. K., & Medina, D. (1996). Organic and inorganic selenium compounds inhibit mouse mammary cell growth in vitro by different cellular pathways. *Cancer Letters*, *107*, 277–284.

Wang, C. L., & Lovell, R. T. (1997). Organic selenium sources, selenomethionine and selenoyeast, have higher bioavailability than an inorganic selenium source, sodium selenite, in diets for channel catfish (*Zctalurus punctatus*). *Aquaculture*, *152*, 223–234.

Wang, J. L., Zhao, B. T., Wang, X. F., Yao, J., & Zhang, J. (2012). Synthesis of selenium-containing polysaccharides and evaluation of antioxidant activity in vitro. *International Journal of Biological Macromolecules*, *51*, 987–991.

Wang, L., Wang, G. Y., Zhang, J. J., Zhang, G. Q., Jia, L., Liu, X. N., et al. (2011). Extraction optimization and antioxidant activity of intracellular selenium polysaccharide by *Cordyceps sinensis* SU-02. *Carbohydrate Polymers*, *86*, 1745–1750.

Wang, W. F., Mai, K. S., Zhang, W. B., Xu, W., Ai, Q. H., Liufu, Z., et al. (2012). Dietary selenium requirement and its toxicity in juvenile abalone *Haliotis discus hannai* Ino. *Aquaculture*, *330–333*, 42–46.

Wang, Y., Chen, J., Zhang, D., Zhang, Y., Wen, Y., Li, L., et al. (2013). Tumoricidal effects of a selenium (Se)-polysaccharide from Ziyang green tea on human osteosarcoma U-2 OS cells. *Carbohydrate Polymers*, *98*, 1186–1190.

Wu, L., Yick, K. L., Ng, S. P., & Yip, J. (2012). Application of the Box–Behnken design to the optimization of process parameters in foam cup molding. *Expert Systems with Applications*, *39*, 8059–8065.

Xu, C., Wang, Y., Jin, M., & Yang, X. (2009). Preparation characterization and immunomodulatory activity of selenium-enriched exopolysaccharide produced by bacterium *enterobacter cloacae* Z0206. *Bioresource Technology*, *100*, 2095–2097.

Yu, J., Cui, P. J., Zeng, W. L., Xie, X. L., Liang, W. J., Lin, G. B., et al. (2009). Protective effect of selenium-polysaccharides from the mycelia of *Coprinus comatus* on alloxan-induced oxidative stress in mice. *Food Chemistry*, *117*, 42–47.

Zhao, L. Q., Chen, Y. L., Ren, S., Han, Y., & Cheng, H. B. (2010). Studies on the chemical structure and antitumor activity of an exopolysaccharide from *Rhizobium* sp. N613. *Carbohydrate Research*, *5*, 637–643.

Zong, A. Z., Cao, H. Z., & Wang, F. S. (2012). Anticancer polysaccharides from natural resources: A review of recent research. *Carbohydrate Polymers*, *90*, 1395–1410.